Molecular dynamics simulations of phase transitions in argon-filled single-walled carbon nanotube bundles under high pressure

K. V. Shanavas and Surinder M. Sharma
High Pressure Physics Division, Bhabha Atomic Research Centre, Mumbai-400 085, India
(Received 8 August 2008; revised manuscript received 9 February 2009; published 16 April 2009)

The behavior of single-walled carbon nanotubes has been investigated under high pressures with the help of classical molecular dynamics simulations in two configurations: when bundles are empty and when argon is present as a pressure transmitting medium. Our calculations show that for the empty tubes, depending on the pressure step, relaxation times, and temperature, several different organizations of collapsed tubes exist for the high-pressure phase above 2.4 GPa. When the nanotubes are filled with argon (as well as surrounded by it), the high-pressure behavior is found to be substantially different. The phase transition shifts to higher pressures as the number of argon atoms inside the nanotubes is increased beyond a critical value and becomes close to 7 GPa for the calculated optimum Ar density. Computed x-ray diffraction patterns of argon-filled nanotubes show that the intensity of the first diffraction peak, which experimentally has been taken as indicative of two-dimensional order in bundles, persists up to higher pressures. We propose that seemingly varied experimental observations in the high-pressure phase transitions of carbon nanotubes are due to the pressure transmitting medium at different densities.

DOI: 10.1103/PhysRevB.79.155425 PACS number(s): 64.70.Nd, 62.25.−g, 02.70.Ns, 62.50.−p

I. INTRODUCTION

Due to many extraordinary properties arising from the unique one-dimensional structure, carbon nanotubes have been subject of intense theoretical and experimental investigations since their discovery.[1] Early theoretical studies had indicated that isolated tubes may be able to withstand large deformations without much irreversible structural modifications.[2] Since then, many experiments have been carried out to understand the behavior of bundles of carbon nanotubes under high pressures. Raman,[3–5] x-ray diffraction,[6,7] and neutron-diffraction[8] measurements have provided evidence for a pressure-induced structural phase transition. In particular, the high-pressure Raman spectroscopic investigations carried out on bundles of single-walled carbon nanotubes (SWCNTs) showed that the peak position of the tangential mode shifts linearly to higher frequencies, with a change in the slope at ~2 GPa. A number of studies also reported the disappearance of the radial breathing mode (RBM) from the spectrum above that critical pressure.[9] X-ray diffraction studies[6,7] showed that at ~1.5 GPa, the (100) diffraction peak associated with the two-dimensional (2D) lattice of the SWCNTs bundles disappears reversibly, if pressure was kept less than 4 GPa. Subsequent computer simulations, using classical molecular dynamics (MD), found that the carbon nanotubes collapse to a ribbonlike structure at low pressures[10,11] and that the collapse pressure decreases with the increase in the tube diameter. It was also shown that the tubes having diameter larger than a critical value would spontaneously collapse at atmospheric pressure. Studies on double-walled carbon nanotubes reported similar results but with higher collapse pressures, as the two tubes support each other.[12,13] Recent first-principles studies, however, have found the behavior of SWCNTs under uniaxial stress (perpendicular to the tube axis) to be nonmonotonous as a function of the tube diameter.[14]

However, these results were not found to be consistent with the observations of a number of other experimental studies.[15–22] *In situ* x-ray diffraction investigations[15] on SWCNTs under quasihydrostatic pressures found that the 2D lattice continues to persist up to ~10 GPa, in contrast to the earlier results. Kawasaki *et al.*[16] compared the effect of the solid and liquid pressure transmitting medium (PTM) on the high-pressure x-ray diffraction patterns and concluded that the penetration of liquid PTM could explain the observed differences in results. Raman spectroscopic studies[17,18] of open-ended SWCNTs using different PTM (paraffin oil, argon, methanol ethanol, etc.) could not observe signatures of any phase transition at low pressures. Instead, they found that the pressure-induced changes in Raman spectra depend significantly on the PTM. Similar PTM dependence is also observed for double-walled tubes as well.[19]

From these results it is clear that for open-ended tubes, the pressure transmitter used in the hydrostatic experiments may enter tubes and affect their high-pressure behavior. Indeed, Rols *et al.*[23] demonstrated that the substantial argon adsorption takes place at the inner walls of SWCNTs. However, theoretical studies so far have treated the carbon nanotubes as empty. Hence, to understand the diverse experimental reports, we have simulated SWCNTs immersed in fluid argon using the classical MD method.

The manuscript is organized as follows. Section II deals with the details of the computational method employed. In Sec. III A we present the results of MD simulations carried out to investigate the nature of collapse in empty SWCNTs under pressure by exploring various parameters that might affect the final structure of the collapsed state. The SWCNT+Ar system is simulated in two parts. In the first part presented in Sec. III B, argon is present only inside the tubes (INT sites) whereas in the second part (Sec. III C) it occupies INT as well as the interstitial channel (IC) sites. In Sec. III D we have tried to compare our results with experimental observations. Section IV gives the conclusions derived from the present investigations.

TABLE I. Parameters for the Lennard-Jones short-range interaction potential (Refs. 25 and 26) between the elements of MD simulation cell.

Atoms	ε (kcal/mol)	σ (Å)
C-C	0.0951	3.473
Ar-Ar	0.2862	3.350
Ar-C	0.2827	3.573

II. COMPUTATIONAL METHOD

Simulations were carried out on (10, 10) arm-chair SWCNTs of diameter 13.59 Å generated using the TUBEGEN (Ref. 24) code. Macrocell used in the simulations consisted of these SWCNTs arranged in a 4×4 two-dimensional hexagonal lattice that were ten graphene unit cells long (24.6 Å) in the z direction. Periodic boundary conditions were applied in all the three directions. The covalent interactions between carbon atoms were modeled by the standard generic macromolecular force field DREIDING,[25] which has been successfully used in many earlier studies.[10,12] Intertube C-C as well as C-Ar and Ar-Ar short-range interactions were of the Lennard-Jones functional form $U(r_{ij})=4\varepsilon[(\sigma/r_{ij})^{12}-(\sigma/r_{ij})^{6}]$ with a 12 Å cutoff. Parameters of L-J potentials are listed in Table I.[25,26]

For our simulations, we have used DL_POLY code with the *NPT* statistical ensemble. The equations of motion were integrated using standard Verlet algorithm with a time step of 1 fs. The temperature (300 K) and the hydrostatic pressure were maintained using the Berendsen thermostat and barostat. The bundles were initially equilibrated at zero pressure and subsequently the pressure was raised in steps, allowing the cell volume to equilibrate for at least 10 ps after each increase. The calculations were carried out on ANUPAM AJEYA supercomputer at Bhabha Atomic Research Centre.

The argon-filled nanotubes for simulations described in Secs. III B and III C were generated by adding a specific and equal number of argon atoms in each of the nanotubes in the macrocell. To remove any memory of starting structures, the system was equilibrated for a long time under ambient conditions.

III. RESULTS AND DISCUSSION

A. High-pressure phases of empty SWCNTs

Although different computer simulations agree on the existence of a transition to a collapsed phase, the exact structure of the daughter phase has not been settled unambiguously.[27,28] Computations using DREIDING potentials on single- and double-walled carbon nanotubes[10,12] observed a herringbone structure whereas studies using Tersoff-Brenner potential[11] found a linear arrangement of similarly deformed tubes at comparable pressures. Energy considerations seemed to favor the linear structure,[27] but the energy differences between the two structures were found to be less than the thermal energy (k_BT) at the temperature of the simulations. It was argued that the precise arrangement of the collapsed nanotubes within a bundle may vary depending on the size of the macrocell, local environment, and compression rate.[28] More recently, the first-principles studies of structural, electronic, and optical properties of collapsed SWCNTs bundles found an in-between configuration which was distinct from both the linear and herringbone structures found previously.[29] Therefore, it is important to understand why different studies yield different results and for these reasons, we have carried out extensive calculations by tuning the control parameters to understand their effect on the high-pressure structure of nanotubes.

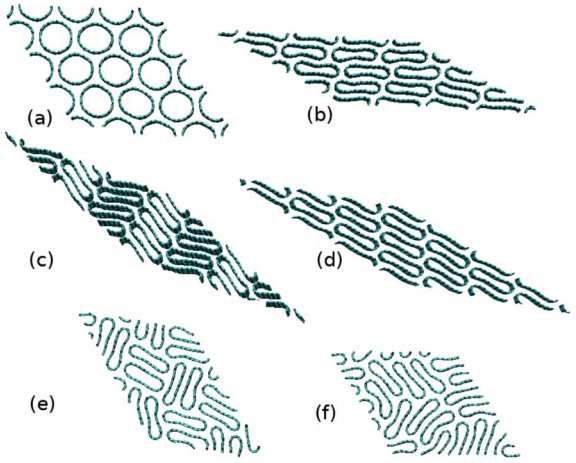

FIG. 1. (Color online) (a) Simulated structure of SWCNTs at 0 GPa and 300 K as viewed along z axis. Other figures represent snapshots of the collapsed phases at 3 GPa. (b) The linear-o and (c) herringbone structures are the result of fine and coarse pressure steps, respectively. (d) Linear-n, (e) basket-weave, and (f) disordered structures are new arrangements observed in our simulations. In agreement with the elastic ring model by Liew *et al.* (Ref. 30), the structures of collapsed tubes show a peanut-shaped deformation under hydrostatic pressure.

The pressure step used to compress the system is an important parameter known to affect transitions under pressure and we carried out a series of simulations to investigate its effect on the behavior of nanotubes. The initial state generated through equilibration of (10, 10) carbon nanotubes at 300 K remains nearly circular as shown in Fig. 1(a). When very fine steps close to 0.1 GPa were used to compress this system, an abrupt volume drop of about 33% was observed at 2.4 GPa, resulting in a new phase with ribbonlike tubes shown in Fig. 1(b) which is similar to the linear structure of Ref. 27. When we used larger compression rates in the range of 1–2 GPa, the herringbone structure [Fig. 1(c)] was obtained, also observed in the earlier studies using DREIDING potentials. Careful inspection of trajectories during the transition to herringbone structure revealed that the deformation of the tubes pass through a transient linear structure in which the tubes are arranged along the [110] direction. At the very final stage of the evolution, the zigzag ordering characteristic of the herringbone sets in. To test whether the thermal fluctuations at 300 K are responsible for stabilizing the herringbone structure, we repeated these simulations at very low temperatures ($\sim$2 K). In this case, we found that a new

TABLE II. Total energies, enthalpies, and volumes of different high-pressure phases given in Fig. 1 at 3 GPa (300 K). Values in parenthesis correspond to differences from the linear-n structure.

Structure	*E*/atom (eV)	*H*/atom (eV)	*V*/atom (Å^3)
Linear-n	7.62	7.79	9.21
Linear-o	7.68	7.86	9.29
	(0.06)	(0.07)	(0.08)
Herringbone	7.70	7.88	9.50
	(0.08)	(0.09)	(0.29)
Basket-weave	7.75	7.93	9.55
	(0.13)	(0.14)	(0.34)
Disordered	7.77	7.95	9.59
	(0.15)	(0.16)	(0.38)

linear structure with a different cell shape and tube arrangement is stable. To differentiate the two linear structures, hereafter we refer the structure of Fig. 1(b) as linear-o and that of Fig. 1(d) as linear-n. Upon increasing the temperature of linear-n slowly to 300 K, the tubes retained the arrangement. Interestingly, still higher-pressure steps (3 GPa) at room temperature resulted in a new phase that has a basket-weave-like ordering with tubes arranged in parallel pairs, almost perpendicular to one another [Fig. 1(e)]. The transition in empty SWCNTs was also found to depend on thermostat and barostat relaxation times used in the simulations. Tubes became disordered [Fig. 1(f)] when relaxation times of 10 ps each were used. Simulations on a smaller $3\times3\times10$ macrocell also yielded the disordered structure similar to Fig. 1(f). In all the cases, the transition is completely reversible; all structures return to the ambient phase with cylindrical tubes upon the release of pressure.

Table II summarizes the relative energies, enthalpies, and volumes per atom for the cases discussed above. We find that the linear-n structure has the lowest energy and although the energy of the linear-o structure is lower than that of the herringbone, the energy difference between these two is within the thermal fluctuations at room temperature. Calculation of volume occupied by the collapsed tubes in different cases indicated that while the tube volume is roughly equal, the interstitial volume increases systematically from linear-n to disordered phases resulting in less compact structures with higher energies, in agreement with the conclusions of Ref. 27. The lower volume (hence, lower energy) of linear-n as compared to the linear-o is probably because of the arrangement of tubes rather than their direction. In the first case, the tubes are arranged such that the tubes point to the empty spaces between the neighbors (along [110] direction), whereas for linear-o the collapsed tubes are arranged end to end.

We carried out simulated annealing on the herringbone structure up to 1000 K, but it did not transform to the lower-energy structures in Fig. 1, indicating that such reconstructions are kinetically hindered up to this temperature. Although our simulations demonstrated the existence of a variety of structures in the high-pressures phase, we feel that Fig. 1 may not represent a complete set of all possible arrangements of the collapsed tubes under pressure. For example, inclusion of nonhydrostatic stresses may lead to still new structures. To sum up, our studies show that the unique structure of nanotubes gives rise to a variety of arrangements for the collapsed tubes and the pressure step plays a vital role in deciding a particular arrangement.

B. SWCNTs with argon at INT sites

To study the high-pressure behavior of carbon nanotubes immersed in a fluid (such that it fills the tube as well as surrounds it), we have simulated argon-filled nanotubes at various argon densities. Choice of argon was partly due to the simplicity of its interatomic interactions (being an inert element, argon interacts with environment through simple van der Waals forces, which could be easily modeled through the Lennard-Jones type of pair potentials) and partly as an effort to understand the recent experiments which used argon as PTM. We believe that the results will be qualitatively similar for any other PTMs which do not chemically react with the carbon atoms of the tubes. However, an important limitation of the present simulations is that the interaction potentials and periodic boundary conditions forbid the expulsion/exchange of argon atoms from within the carbon nanotubes, whereas in experiments this may occur due to defects in the tube walls or the absence of end caps.

In a typical high-pressure experiment, the pressure cell containing the sample is kept immersed in a bath to fill the sample region with PTM. Since computer representation of such a scenario is forbidden by present interaction potentials, we have instead carried out several simulations at different densities to explore the effect of PTM on the behavior of nanotubes. Rols *et al.*[23] studied argon adsorption on open-ended SWCNTs through thermodynamics and neutron-diffraction experiments and have proposed the following adsorption scenario. The inner walls of the nanotubes and the groove sites on the outer surface of the bundle are populated first followed by the filling of the axial sites inside the tubes and remainder of the outer bundle surface. Although direct evidence was limited, a few intertubular sites seemed to be progressively populated as a function of the Ar chemical potential.[23] Interestingly, recent studies on rubidium-intercalated SWCNTs show that Rb ions prefer IC sites at very low stoichiometry. At higher Rb levels, IC sites become unfavorable and INT and bundle surface sites begin to get occupied.[31] Based on these propositions, we have carried out two sets of simulations. In the first set, presented in this section, IC sites were neglected and argon was restricted to INT sites. The second set of simulations, in which both INT and IC sites were populated, are presented in Sec. III C. Note that due to the requirement of an infinite periodic system, we have ignored the outer surfaces of the bundle altogether, but those sites are unlikely to affect the high-pressure behavior of the bundle.

Figure 2 shows the computed variation in energy/atom with the argon number density. It decreases linearly for low argon densities to become minimum close to 60, which would correspond to optimum filling under ambient condi-

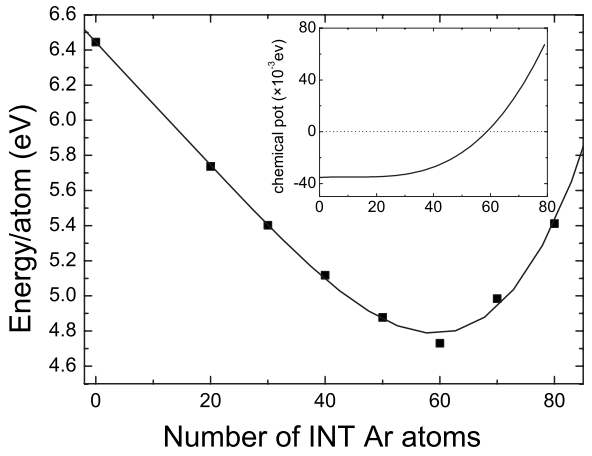

FIG. 2. Variation in the energy with the number of argon atoms at INT sites fitted with a fourth-order polynomial (solid line). The inset shows the derivative of total energy with respect to the argon number density. The horizontal dotted line marks the zero chemical potential.

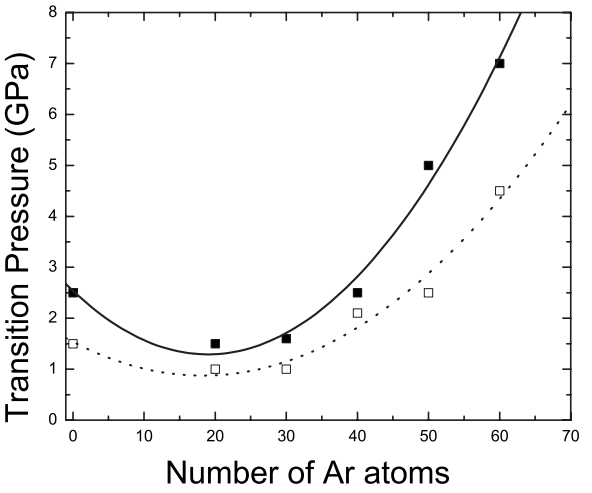

FIG. 4. Variation in the transition pressure with the number of argon atoms per nanotube. Closed and open symbols represent the results during compression and decompression, respectively. Solid and dotted lines indicate a quadratic fit to the transition pressure.

tions (the negative value of the chemical potential at lower densities indicate that these tubes are under filled). Although in experiments under ambient conditions tubes will be filled to an optimal value, one can certainly generate the under or over filled tubes by varying equilibration time and density of argon atoms in the bath.[23]

SWCNTs with argon densities varying from 0 to 70 atoms/tube were subjected to increasing pressures in steps of 1 GPa (or 0.1 GPa close to phase transitions) up to 10 GPa. Pressure was then released back to zero in a similar manner. As can be seen from the few representative cases given in Fig. 3, depending on the degree of filling of the tubes, the volume decreases discontinuously at some pressure, marking a structural phase transition of the first order. For a particular case of 40 atoms/tube, however, we observe multiple volume drops at 2.5, 5.4, and 8.5 GPa. Inspection of the intermediate structures revealed that argon undergoes structural modifications of different compactness, forcing the enveloping nanotubes to collapse in stages. Multiple phase transitions similar to this case have also been observed in experiments,[20] when nanotubes filled with fullerenes were subjected to high pressures. Another important observation is that as the density increases, the change in volume at the transition becomes smaller. Hence, at higher argon densities the transformation may appear gradual and will probably explain the recent resonant Raman spectroscopic studies[17] on open-ended nanotubes using argon PTM, which found the structural changes to be progressive rather than abrupt.

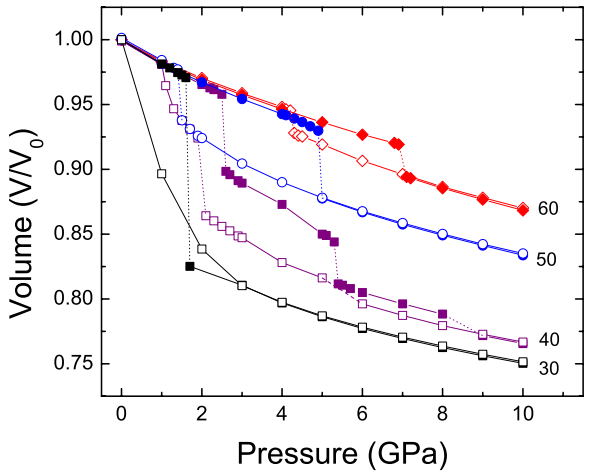

FIG. 3. (Color online) Pressure-volume behavior for single-walled carbon nanotubes containing 30, 40, 50, and 60 argon atoms per tube. Closed symbols represent compression and open symbols denote results on the release path of the pressure.

Computed variation in the transition pressure (P_T) in Fig. 4 shows that when the number of argon atoms per nanotubes is increased beyond a critical value (~40 argon atoms/tube), the P_T increases almost quadratically and at the optimum density (60 atoms/tube), it is close to 7 GPa. During the release of pressure, a similar curve is followed; although with lower values of P_T, representing the well-known hysteresis in the first-order phase transitions. The lowering of the transformation pressure below 40 atoms/tube is puzzling because intuitively one would expect that when an empty tube is filled with some fluid, it will become less compressible and thus withstand higher stresses before collapse. This seemingly unusual result can be rationalized as follows.

As the tubes are quite incompressible along the axial direction, the effect of the applied stress is felt primarily in the radial direction. When it is filled with argon, due to van der Waals interaction between the argon and carbon atoms, the tubes would experience an additional force which—due to the cylindrical symmetry—will also be directed along the radius of the tubes. Van der Waals interaction is repulsive at short distances [below a radius r_{min} (Ref. 32)] but is weakly attractive above r_{min}. As a result, when too few argon atoms are inside the tubes, the average distances between argon atoms and tube walls are greater than the r_{min} and the average interaction is attractive. This effective attractive force adds to the external pressure and increases the inward stress on the tube, collapsing it at a lower pressure. But when the

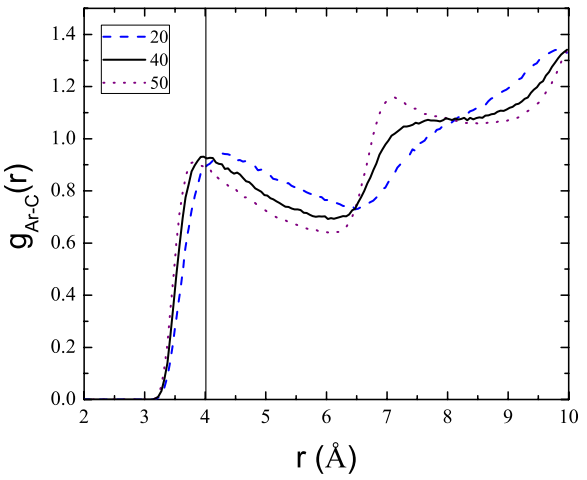

FIG. 5. (Color online) Computed Ar-C pair-correlation functions for different argon atomic densities. As this density increases, the peaks move to lower r values. The vertical line corresponds to r_{min} of the Lennard-Jones potential used in our simulations.

argon density inside the tubes becomes large enough to have the average argon-carbon distance less than r_{min}, the interactions become repulsive which in turn helps the tubes withstand higher pressures. Thus the collapse pressure increases. Figure 5 shows that for 20 atoms/tube, the Ar-C pair distribution function $[g(r)]$ peaks above r_{min} and for higher Ar densities, the maximum shifts toward lower r values accompanied by an increase in the transition pressure. It would be interesting to test these results by carrying out experiments with carbon nanotubes filled with pressure transmitter at lower densities.

Interestingly, the zero pressure structures of SWCNTs with INT argon (Fig. 6) resemble multiwalled nanotubes, although argon atoms are quite disordered. Similar local partial ordering and shell formation of the pressure medium around the nanotubes is supported by *ab initio* studies, which also find it to have a strong impact on pressure transmission.[19] Similar to our results beyond the critical argon density, computer simulations on double-walled tubes[12] found transition pressures to be higher as the two walls support each other. To compare, the P_T for a double-walled nanotube of type (5,5)@(10,10) is ~18 GPa (Ref. 12) whereas for optimally filled SWCNTs it is ~7 GPa.

High-pressure structures of argon-filled nanotubes are also quite varied (Fig. 7). Up to 40 atoms/tube, the collapsed tubes adopt linear arrangements similar to those of empty

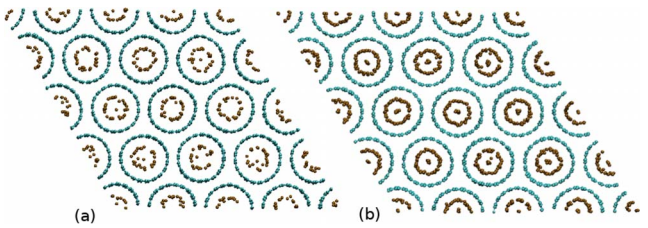

FIG. 6. (Color online) Snapshots of the simulation cell containing single-walled carbon nanotubes filled with (a) 40 and (b) 60 argon atoms/tube at INT sites at 0 GPa and 300 K show argon forming cylindrical structures inside the tubes.

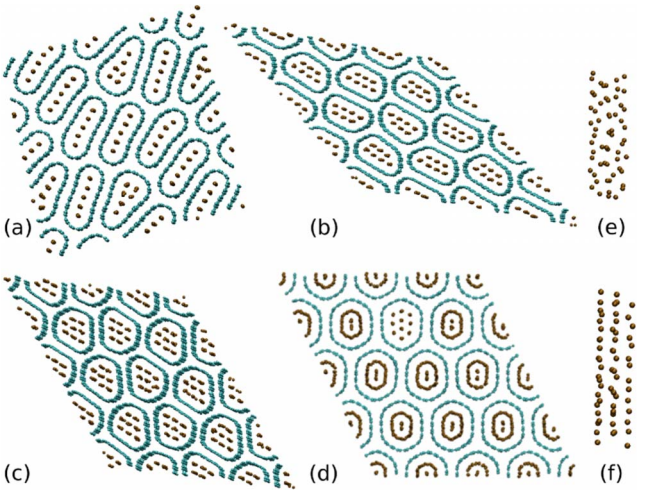

FIG. 7. (Color online) High-pressure phases of nanotubes at 10 GPa with (a) 40, (b) 50, (c) 60, and (d) 70 argon atoms per tube. Side view argon atoms inside a single nanotube for 60 atoms/tube is shown in (e) at 0 GPa and (f) at 10 GPa.

tubes and argon atoms form a linear array parallel to the walls of the tubes. The intermediate densities shown in Figs. 7(b) and 7(c) represent a transitional regime in which faceting emerges along with the limited collapse of the tubes. All these structures prefer an arrangement similar to Fig. 1(d). At densities over 70 atoms/tube, the forces favor faceting and nanotubes become "polygonized." It is interesting to note that in many early studies, authors had argued in favor of polygonization over collapse and our simulations show that indeed both regimes exist when a PTM is present in the system. Figures 7(e) and 7(f) demonstrate the ordering of argon along z direction inside a single nanotube across the phase transition.

C. SWCNTs with argon at INT and IC sites

To calculate the minimum-energy configuration, we fixed the INT argon at 50 atoms/tube and varied the IC site den-

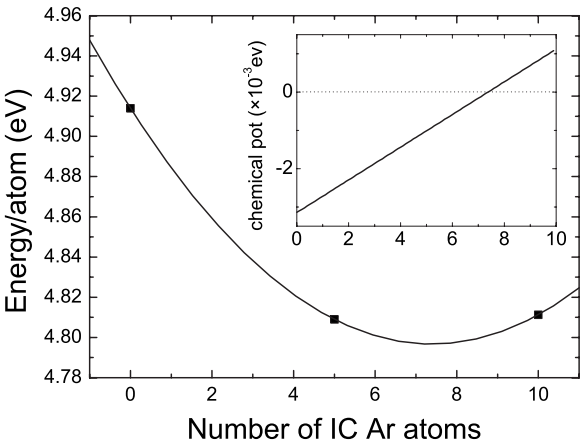

FIG. 8. Variation in the total energy with the number of argon atoms in the intertubular region. Argon inside the tubes is kept fixed at 50 atoms/tube. The chemical potential in the inset shows essentially linear behavior.

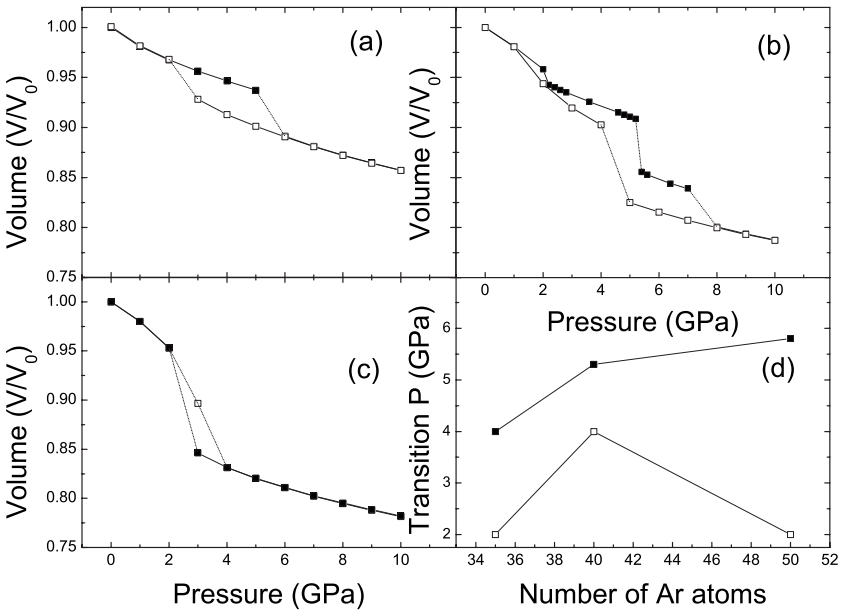

FIG. 9. (a) *P-V* behavior of argon-filled carbon nanotubes with 50 atoms inside (INT sites) and 7 atoms in the interstitial (IC sites). Similar curves are plotted for (b) 40 INT+7 IC and (c) 35 INT+7 IC cases. (d) Variation in the transition pressure with the total number of argon atoms.

sity. A value lower than the optimum INT density (Sec. III B) was chosen because the additional stress due to the presence of argon at IC sites would increase the chemical potential at INT sites and would lower the optimum value.[33] Minimum energy was found to occur when alternate IC sites are filled with about 7 atoms per tube (Fig. 8). As argon atoms at IC sites are arranged as a one-dimensional chain along z axis, for more than 7 atoms/tube, Ar-Ar distances become less than $r_{\min}$ (Ref. 32) (~3.76 Å), making the interaction repulsive.

As we can see from pressure-volume curves given in Fig. 9, argon atoms present outside the tubes further affect the behavior of the tubes. A significant observation is that in all cases studied, the transition pressures are higher. We feel that the reduced intertubular space diminishes fluctuations that lead to the collapse of nanotubes and hence increases the transition pressure. The transition is abrupt for the case of 50+7 (INT+IC) atoms/tube, whereas for 35+7 it is spread over a wider range of pressures. Similar to the case without IC atoms, there are multiple transitions for 40+7, though the largest drop is found at 5.3 GPa instead of 2.5 GPa.

The structures of collapsed tubes are also different when argon is present at IC sites. At ambient pressures, IC argon atoms form a triangular lattice [Fig. 10(a)]. At 10 GPa, the collapsed tubes are arranged in layers and tubes in the neighboring layers form an angle of ~70° with each other and argon atoms, which were initially arranged on an approximate equilateral triangular lattice of side 17 Å, now form bilateral triangles with two sides of 17 Å and one of 13 Å.

D. Powder x-ray diffraction patterns of nanotubes

To make a contact with the experiments, we have calculated the x-ray diffraction patterns for the simulated structures.[34] Under ambient conditions, the observed diffraction patterns show (100) as the dominant peak. The next most intense peak (at $q \sim 1.0$ Å^{-1} for our system) is found to be almost one order of magnitude weaker. In a diamond-anvil cell, only the first diffraction peak was observed even in synchrotron-based experiments, which was attributed to the 2D hexagonal order of the tubes in the bundles. This peak disappears at the transition, which was interpreted as the loss of the translational order. The calculated diffraction profile in Fig. 11(a) for the equilibrated ambient nanotubes bundle shows features which are in a very good agreement with that of experimental patterns.[35] The diffraction pattern of herringbone structure of empty SWCNTs [Fig. 11(b)] shows loss of intensity of (100) peak by several orders of magnitude consistent with the observations in the high-pressure experiments. Other structures of the linearized tubes shown in Fig. 1 also have equally weak-computed intensities, making them indistinguishable with reference to presently published x-ray results. However, as is evident from Fig. 1, the translation order is not completely lost in these structures and in fact, calculated patterns show subtle differences. So, in principle, more sensitive experiments may be able to identify the physically realized structure; but this would require considerable experimental improvements to substantially reduce the background arising from diamonds and other sources.

The loss of the diffracted intensity of the first peak with argon at INT sites[36] is not as dramatic as empty SWCNTs

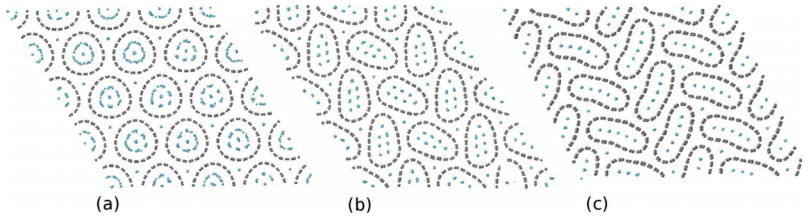

FIG. 10. (Color online) Snapshots of simulation containing SWCNTs and argon at INT+IC sites. (a) 50+7 argon atoms/tube at 0 GPa, (b) 50+7 atoms/tube at 10 GPa, and (c) 40+7 atoms/tube at 10 GPa.

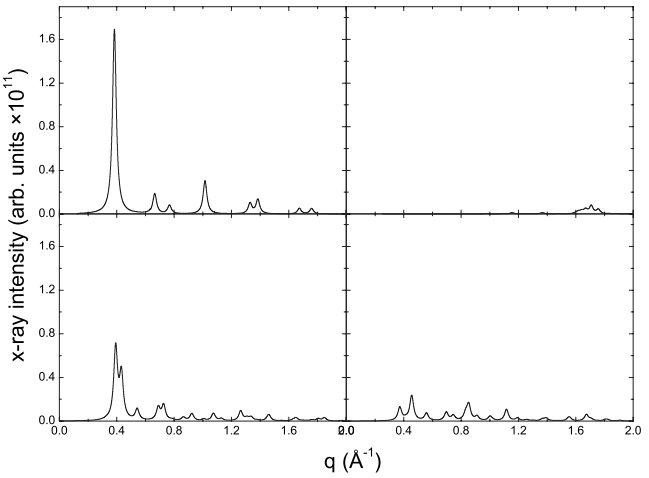

FIG. 11. Calculated x-ray diffraction patterns of SWCNTs (a) empty tubes at 0 GPa and (b) herringbone at 10 GPa. Patterns for argon-filled nanotubes with argon at INT sites (c) and at INT+IC sites (d) are calculated at 10 GPa. So as to facilitate the interpretation of experimental results, the intensity scale has been kept the same.

[Fig. 11(c)]. The remnant order after collapse is still appreciable to produce intense peaks. However, when argon is present at INT as well as IC sites the diffraction signal reduces substantially. Since the transition pressure in this case is higher, the inferred loss of 2D order in the filled SWCNTs would take place at higher pressures when compared to that for the empty tubes. These results provide a rational understanding of the results of Ref. 13 as those tubes were prepared by arc-discharge method and hence may have missing end caps and could be filled in a manner representative of Sec. III C.

We may also add that though for the present comparison, the form factors of Ar were set to zero, the inclusion of scattering from Ar shows the emergence of ordered structures of Ar in SWCNTs. Therefore, it may be interesting to carry out such experiments to determine the ordering of Ar atoms in SWCNTs under high pressures.

IV. SUMMARY

To summarize, our classical MD simulations have shown that for SWCNTs at high pressures several competing kinetically separated arrangements of the collapsed tubes are possible. We have also shown that compared to the empty tubes, nanotubes bundles filled with argon atoms behave quite differently under pressure. As the density of argon atoms at INT sites is increased beyond the critical value of 40 atoms/tube, the pressure of transformation increases. At the critical density, multiple volume changes are observed as argon atoms undergo ordering in stages. Interestingly, at low argon concentrations, the nanotubes are found to adopt a collapsed structure whereas at high concentrations they become faceted. Calculated diffraction patterns imply that for empty SWCNTs the diffraction experiments would show loss of the first diffraction peak across the phase transition ~2.4 GPa. In contrast, for Ar-filled SWCNTs, the pressure of transformation, as determined through the loss of diffraction signal, would be much higher. Ar atoms show the emergence of order at high pressures and these results should encourage further experimental investigations.

ACKNOWLEDGMENTS

The authors are thankful to Nandini Garg and K. K. Pandey for their useful discussions.

[1] S. Iijima, Nature (London) **354**, 56 (1991).
[2] S. Iijima, C. Brabec, A. Maiti, and J. Bernholc, J. Chem. Phys. **104**, 2089 (1996).
[3] U. D. Venkateswaran, A. M. Rao, E. Richter, M. Menon, A. Rinzler, R. E. Smalley, and P. C. Eklund, Phys. Rev. B **59**, 10928 (1999).
[4] M. J. Peters, L. E. McNeil, J. P. Lu, and D. Kahn, Phys. Rev. B **61**, 5939 (2000).
[5] J. Sandler, M. S. P. Shaffer, A. H. Windle, M. P. Halsall, M. A. Montes-Morán, C. A. Cooper, and R. J. Young, Phys. Rev. B **67**, 035417 (2003).
[6] J. Tang, L.-C. Qin, T. Sasaki, M. Yudasaka, A. Matsushita, and S. Iijima, Phys. Rev. Lett. **85**, 1887 (2000).
[7] S. Karmakar, S. M. Sharma, P. V. Teredesai, D. V. S. Muthu, A. Govindaraj, S. K. Sikka, and A. K. Sood, New J. Phys. **5**, 143 (2003).
[8] S. Rols, I. N. Gontcharenko, R. Almairac, J. L. Sauvajol, and I. Mirebeau, Phys. Rev. B **64**, 153401 (2001).
[9] W. Yang, R. Z. Wang, X. M. Song, B. Wang, and H. Yan, Phys. Rev. B **75**, 045425 (2007).
[10] J. A. Elliott, J. K. W. Sandler, A. H. Windle, R. J. Young, and M. S. P. Shaffer, Phys. Rev. Lett. **92**, 095501 (2004).
[11] X. H. Zhang, D. Y. Sun, Z. F. Liu, and X. G. Gong, Phys. Rev. B **70**, 035422 (2004).
[12] V. Gadagkar, P. K. Maiti, Y. Lansac, A. Jagota, and A. K. Sood, Phys. Rev. B **73**, 085402 (2006).
[13] X. Ye, D. Y. Sun, and X. G. Gong, Phys. Rev. B **75**, 073406 (2007).
[14] D. Chen, T. Sasaki, J. Tang, and L.-C. Qin, Phys. Rev. B **77**, 125412 (2008).
[15] S. M. Sharma, S. Karmakar, S. K. Sikka, P. V. Teredesai, A. K. Sood, A. Govindaraj, and C. N. R. Rao, Phys. Rev. B **63**, 205417 (2001).
[16] S. Kawasaki, Y. Matsuoka, T. Yokomae, Y. Nojima, F. Okino, H. Touhara, and H. Kataura, Phys. Status Solidi B **241**, 3512 (2004).
[17] A. Merlen, N. Bendiab, P. Toulemonde, A. Aouizerat, A. San Miguel, J. L. Sauvajol, G. Montagnac, H. Cardon, and P. Petit, Phys. Rev. B **72**, 035409 (2005).
[18] A. Merlen, P. Toulemonde, N. Bendiab, A. Aouizerat, J. L. Sauvajol, G. Montagnac, H. Cardon, P. Petit, and A. San Miguel, Phys. Status Solidi B **243**, 690 (2006).

[19] P. Puech, E. Flahaut, A. Sapelkin, H. Hubel, D. J. Dunstan, G. Landa, and W. S. Bacsa, Phys. Rev. B **73**, 233408 (2006).
[20] Ch. Caillier, D. Machon, A. San-Miguel, R. Arenal, G. Montagnac, H. Cardon, M. Kalbac, M. Zukalova, and L. Kavan, Phys. Rev. B **77**, 125418 (2008).
[21] K. Gao, R. C. Dai, Z. M. Zhang, and Z. J. Ding, Solid State Commun. **147**, 65 (2008).
[22] M. Yao, Z. Wang, B. Liu, Y. Zou, S. Yu, W. Lin, Y. Hou, S. Pan, M. Jin, B. Zou, T. Cui, G. Zou, and B. Sundqvist, Phys. Rev. B **78**, 205411 (2008).
[23] S. Rols, M. R. Johnson, P. Zeppenfeld, M. Bienfait, O. E. Vilches, and J. Schneble, Phys. Rev. B **71**, 155411 (2005).
[24] http://turin.nss.udel.edu/research/tubegenonline.html/
[25] S. L. Mayo, B. D. Olafson, and W. A. Goddard III, J. Phys. Chem. **94**, 8897 (1990).
[26] R. E. Tuzun, D. W. Noid, B. G. Sumpter, and R. C. Merkle, Nanotechnology **7**, 241 (1996).
[27] X. H. Zhang, Z. F. Liu, and X. G. Gong, Phys. Rev. Lett. **93**, 149601 (2004).
[28] J. A. Elliott, J. K. W. Sandler, A. H. Windle, R. J. Young, and M. S. P. Shaffer, Phys. Rev. Lett. **93**, 149602 (2004).
[29] X. Yang, G. Wu, J. Zhou, and J. Dong, Phys. Rev. B **73**, 235403 (2006).
[30] K. M. Liew and Y. Sun, Phys. Rev. B **77**, 205437 (2008).
[31] N. Bendiab, A. M. Saitta, R. Aznar, J. L. Sauvajol, R. Almairac, I. Mirebeau, and G. Andre, Phys. Rev. B **78**, 104108 (2008).
[32] r_{min} corresponds to the distance, where force becomes zero. It is related to σ as $r_{min}=2^{1/6}\sigma$. From Table I, $\sigma=3.573$ Å for C-Ar and hence $r_{min}=4.01$ Å.
[33] Equilibration of a 60+7 bundle at ambient pressure resulted in an increase in volume justifying this argument.
[34] M. S. Somayazulu, S. M. Sharma, and S. K. Sikka, Phys. Rev. Lett. **73**, 98 (1994).
[35] A. Thess, R. Lee, P. Nikolaev, H. Dai, P. Petit, J. Robert, C. Xu, Y. H. Lee, S. G. Kim, A. G. Rinzler, D. T. Colbert, G. E. Scuseria, D. Tomanek, J. E. Rischer, and R. E. Smalley, Science **273**, 483 (1996).
[36] Diffraction pattern is from carbon alone. Effect of argon lattice is removed by setting argon form factors to be zero.